JOURNAL OF NEUROTRAUMA 28:565–578 (April 2011)

DOI: 10.1089/neu.2010.1533

Effect of Vascular Endothelial Growth Factor Treatment in Experimental Traumatic Spinal Cord Injury: *In Vivo* Longitudinal Assessment

Laura M. Sundberg, Juan J. Herrera, and Ponnada A. Narayana

Abstract

Vascular endothelial growth factor (VEGF) is thought to provide neuroprotection to the traumatically injured spinal cord. We examined whether supplementing the injured environment with $VEGF_{165}$ via direct intraspinal injection into the lesion epicenter during the acute phase of spinal cord injury (SCI) results in improved outcome. The effect of treatment was investigated using longitudinal multi-modal magnetic resonance imaging (MRI), neurobehavioral assays, and end-point immunohistochemistry. We observed on MRI that rats treated with $VEGF_{165}$ after SCI had increased tissue sparing compared to vehicle-treated animals at the earlier time points. However, these favorable effects were not maintained into the chronic phase. Histology revealed that $VEGF_{165}$ treatment resulted in increased oligodendrogenesis and/or white matter sparing, and therefore may eventually lead to improved functional outcome. The increase in spared tissue as demonstrated by MRI, coupled with the possible remyelination and increased neurosensory sensitivity, suggests that $VEGF_{165}$ treatment may play a role in promoting plasticity in the sensory pathways following SCI. However, VEGF-treated animals also demonstrated an increased incidence of persistent allodynia, as indicated on the von Frey filament test.

Key words: behavioral assays; diffusion tensor imaging; magnetic resonance imaging; spinal cord injury; vascular endothelial growth factor

Introduction

Exogenous administration of vascular endothelial growth factor (VEGF) to the traumatically injured spinal cord has been recently investigated as a potential therapy. VEGF is a pro-angiogenic growth factor that also has demonstrated neuroprotective effects (Ferrara et al., 2003; Rosenstein and Krum, 2004; Storkebaum et al., 2004). VEGF has been investigated in models of spinal cord injury (SCI) and stroke with mixed results. Some studies demonstrated that VEGF treatment resulted in improvement after injury (Facchiano et al., 2002; Patel et al., 2009; Widenfalk et al., 2003), while other studies have found that VEGF treatment exacerbated CNS injury (Benton and Whittemore, 2003; Zhang et al., 2000).

The VEGF family consists of seven members: VEGF-A, VEGF-B, VEGF-C, VEGF-D, VEGF-E, VEGF-F, and placental growth factor (PLGF; Ferrara et al., 2003; Otrock et al., 2007; Tammela et al., 2005). VEGF-A, the most studied and characterized member of the VEGF family, has additionally been shown to have neuroprotective effects and encourage neuronal cell growth (Ferrara et al., 2003; Rosenstein and Krum, 2004; Storkebaum et al., 2004). The VEGF-A family can be further subdivided into at least six isoforms of varying amino acid numbers: $VEGF_{121}$, $VEGF_{145}$, $VEGF_{165}$, $VEGF_{183}$, $VEGF_{189}$, and $VEGF_{206}$. Of these, $VEGF_{121}$, $VEGF_{165}$, and $VEGF_{189}$ are the major forms secreted by most cells (Tammela et al., 2005), and $VEGF_{165}$ is the most abundant and biologically active (Zachary, 2005). A previous study demonstrated that endogenous levels of $VEGF_{165}$ are significantly decreased after SCI (Herrera et al., 2009), and therefore supplementing the spinal cord with exogenous VEGF may help in the recovery process. These characteristics make $VEGF_{165}$ an attractive choice for treating injury, yet recent studies attempting to exploit this specific growth factor have produced conflicting results. Benton and Whittemore demonstrated that rats that received an intraspinal injection of $VEGF_{165}$ at 72 h post-SCI demonstrated a significant increase in vascular permeability, extensive infiltration of leukocytes into the spinal cord, and exacerbation of lesion volume compared to vehicle-treated animals at 6 weeks post-injury (Benton and Whittemore, 2003). These results prompted the

Department of Diagnostic and Interventional Imaging, University of Texas Medical School at Houston, Houston, Texas.

authors to conclude that administration of $VEGF_{165}$ may aggravate SCI, likely due to its ability to render vasculature permeable. In contrast, other studies have indicated that $VEGF_{165}$ treatment after injury results in a significant improvement in outcome. Widenfalk and colleagues found that animals treated with a single injection of $VEGF_{165}$ into the spinal cord immediately after injury had significantly improved behavior up to 6 weeks after surgery compared to controls, as well as an increased amount of spared tissue when compared to both angiostatin-treated and control animals (Widenfalk et al., 2003). These beneficial effects seen with the acute delivery of $VEGF_{165}$ were attributed to the protection and repair of blood vessels, decreased apoptosis, and potentially protective effects on other cells. Another study by Facchiano and associates also demonstrated that following SCI, animals receiving $VEGF_{165}$ treatment by direct, acute injection exhibited a 300% increase in newly formed vessels, and had a significant reduction in the extent of retrograde corticospinal tract axonal degeneration with evidence of axonal regeneration (Facchiano et al., 2002). These results collectively provide evidence that is consistent with the hypothesis that $VEGF_{165}$ exerts both vascular and neuroprotective effects after CNS injury.

The goal of this study was to attempt to resolve some of the conflicting results from previous studies by determining the effect of exogenous $VEGF_{165}$ treatment in the acute phase of SCI. To accomplish this, extensive evaluations of the acute and long-term effects of treatment were characterized *in vivo* using a longitudinal multi-modal approach that includes magnetic resonance imaging (MRI) and neurobehavioral tests in the same group of animals. Finally, end-point histological assessments were performed.

Methods

The protocol used in this study was reviewed and approved by the Institutional Animal Welfare Committee, and the guidelines provided in National Institutes of Health (NIH) Guide for the Care and Use of Laboratory Animals were followed.

Animals and spinal cord injury procedure

A total of 30 adult male Sprague-Dawley rats (300–320 g) were used in these studies. The animals were divided into two groups ($n = 15$/group): group 1 animals were treated with $VEGF_{165}$ that was injected directly into the spinal cord, and group 2 animals received an injection of sterile saline (vehicle). The surgical procedures were performed as previously described (Sundberg et al., 2010). Briefly, the animals were anesthetized with isoflurane, intubated, and maintained under anesthesia with a mixture of isoflurane, oxygen, and air that was administered through a rodent ventilator (model 683; Harvard Apparatus, Holliston, MA). A laminectomy was performed at thoracic level 7 (T7), and a 150-kdyn force was delivered to the exposed spinal cord using an Infinite Horizon Impactor (Precision Systems and Instrumentation, LLC, Lexington, KY). Immediately following SCI, a single 1.5-μL dose of either human recombinant $VEGF_{165}$ (4 μg/mL, cat. no. 293-VE; R&D Systems, Minneapolis, MN) or sterile saline was injected into the lesion epicenter via a glass pulled-tip pipette driven by a picospritzer (Parker Hannifin Corporation, Fairfield, NJ). The needle tip was inserted 1 mm from the surface of the spinal cord. We used the same concentration of $VEGF_{165}$ that was employed in a previous study (Widenfalk et al., 2003). Further reference to VEGF in this article refers solely to the $VEGF_{165}$ isoform.

A 11×35-mm rectangular radio frequency (RF) coil was implanted over the spinal column, centered on the site of injury (Deo et al., 2006; Fenyes and Narayana, 1998; Sundberg et al., 2010), held in place with two sutures, and tuned to the operating frequency of the MRI scanner. The overlying muscles were sutured and the skin was closed. During the MRI scans the RF coil was inductively coupled to a 35×40-mm external surface coil that was placed under the animal's back.

The animals received subcutaneous injections of enrofloxacin (Baytril-100; 100 mg/mL, 2.5 mg/kg; Bayer Healthcare LLC Animal Division, Shawnee Mission, KS) twice a day for 3–5 days, and buprenorphine (0.01 mg/kg; Hospira, Inc., Lake Forest, IL) and saline twice daily for 5 days. Their bladders were manually voided twice daily until the return of spontaneous urination. The animals were housed in pairs in plastic cages, had free access to food and water, and were maintained on a 12-h light/dark cycle.

Animal MRI preparation

The animals underwent spinal cord MRI on post-surgery days 7, 14, 28, 42, and 56. They were intubated and anesthesia was maintained with the Harvard Apparatus rodent ventilator. The respiration and rectal temperature were continuously monitored throughout the experiments using a physiologic monitoring unit (model 1025; SA Instruments, Inc., Stonybrook, NY), and the oxygen levels and heart rate were tracked with a pulse oximeter (model 8600V; Nonin Medical Inc., Plymouth, MN). Throughout the scan, the animal's body temperature was maintained at 37°C with a feedback controlled heating system (model 11007B, SA Instruments).

MRI protocol

All MR studies were carried out with a URS 70/30 horizontal bore 7T MRI scanner (Bruker Biospec, Karlsruhe, Germany) as previously described (Sundberg et al., 2010). High-resolution images were acquired using the rapid acquisition by relaxation enhancement (RARE) sequence. Thirty-five 1-mm-thick contiguous and interleaved axial slices were acquired using the following parameters: RARE factor = 4, $TE_1/TE_2/TR = 21.2/63.6/3150$ msec, image matrix = 256×256, square FOV = 2.62 cm.

Diffusion tensor imaging (DTI) was used in these studies to evaluate the white matter fiber tracts. The geometry that was utilized was identical to that used in the RARE sequence. DTI was performed using a spin echo echo planar imaging (EPI) readout sequence with 4 shots, TR/TE = 3000 msec/39.73 msec, receiver bandwidth of 200 kHz, a gradient encoding scheme with 21 positive and negative encoding directions that was balanced and unbiased (42 gradient encoding directions total; Madi et al., 2005), acquisition matrix of 128×128, and images were reconstructed to 256×256.

Evaluation of MRI lesion volume

The RARE images were used to identify and quantify lesion volumes. In the acute phase of SCI, edema appears bright

(hyperintense) and hemorrhage appears dark (hypointense) on T2-weighted MRI. However, in the chronic stages of injury, hyperintense lesions are associated with demyelination and hypointense lesions are associated with necrosis (Weirich et al., 1990). Image-Pro Plus 5.1 software (Media Cybernetics, Inc., Silver Spring, MD) was used for the lesion volume analysis. Individual intensity thresholds for hypointense and hyperintense lesions were previously established by analyzing data from uninjured animals (Sundberg et al., 2010). The thresholds were applied to the spinal cord and the total area of hyper- and/or hypointense lesion was recorded for each of the image slices. The lesion volume was calculated for each image slice, and the total lesion volume for the hyper- and hypointense lesions was determined by summing the volumes for all MRI image slices. Lesion volumes were assessed at each time point in order to evaluate the temporal evolution of injury.

DTI data processing

Diffusion-weighted images (DWI) were post-processed using a processing pipeline that was developed under IDL (ITT Visual Information Solutions, Boulder, CO) to minimize ghosting and noise artifacts (Bockhorst et al., 2010a, 2010b, 2008). Briefly, a digital tuning program corrected the ghosts in the time domain (Ye and Xiang, 2007), then the corrected data were reconstructed using the FRECO macro in ParaVision on the Bruker MRI scanner. The ghosted magnitude images were then replaced by the unghosted images, cropped to a 71×71 matrix to reduce the amount of data processing, and the data were filtered using a Rician filter (Hahn et al., 2004, 2005). The extrameningeal tissues were manually cropped using MRIcro (http://www.cabiatl.com/mricro/mricro/index.html), and this mask was applied to images acquired with all other encoding directions and to the b0 images (images acquired without the application of diffusion gradients) for spinal cord extraction. The diffusion-weighted images were warped to the corresponding b0 images using AIR (align_warp, 3D, model 2; Woods et al., 1998) to minimize image distortions by the eddy currents induced by strong diffusion gradients. Finally, the data were exported to DTI Studio (Jiang et al., 2006; http://cmrm.med.jhmi.edu/). All the steps, aside from the application of the mask, were fully automatic and were processed as batch jobs.

Evaluation of white matter fiber tracts

Fractional anisotropy (FA), transverse diffusivity (λ_T), and longitudinal diffusivity (λ_L) maps were generated using DTI Studio, and the "ROI Manager" of ImageJ software (http://rsb.info.nih.gov/ij/) was used for region-of-interest (ROI) analysis for each of the DTI measures. Methods described previously (Deo et al., 2006; Sundberg et al., 2010) were used to determine values for each of the DTI measures in specific regions within the spinal cord white matter. Briefly, elliptical ROIs were placed in the ventral, dorsal, and right and left lateral white matter regions, and the DTI measures were recorded for each area.

A total of 21 mm of spinal cord tissue was assessed and divided into regions as previously detailed (Sundberg et al., 2010). For the DTI analysis only, the epicenter region was not included because the loss of tissue architecture made it nearly impossible to distinguish between gray and white matter.

Neurobehavioral assays

The animals underwent neurobehavioral assays of open-field locomotion (Basso et al., 1995), inclined plane performance (Rivlin and Tator, 1977), grid walk (Bresnahan et al., 1987), von Frey filament test (Peng et al., 2006), and measures of activity using the Photobeam Activity System (PAS) with Flexfield (San Diego Instruments, Inc., San Diego, CA) computerized activity boxes (Mills et al., 2001). All behavioral assays were performed on the same days as the MRI scans, prior to the administration of anesthesia. A complete description of the assays is provided in Sundberg and colleagues (2010).

Tissue processing and immunohistological staining

To correlate with the final DTI measures, tissue was labeled with antibodies to phosphorylated neurofilament and oligodendrocytes/myelin. After the final MRI scan on day 56, the animals were transcardially perfused with 0.1 M phosphate-buffered saline (PBS) followed by 4% paraformaldehyde. The spinal cords were removed and post-fixed overnight in 4% paraformaldehyde, then immersed in 30% sucrose in PBS for 2–3 days at 4°C. The spinal cords were coronally sectioned at 35 μm using a cryostat (Leica CM1800; Leica, Bannockburn, IL) and stored at −20°C in tissue-storing media.

We examined sections ($n = 8$/animal) from areas that were 0.5 mm rostral and 0.5 mm caudal to the injury epicenter. Tissue sections were processed as free-floating and incubated in the following primary antibodies: neurofilament 200-kD protein (SMI-31R, 1:1000; Covance Inc., Princeton, NJ), and oligodendrocytes/myelin (MAB 328, 1:1200; Millipore, Billerica, MA). Primary antibodies were diluted with blocking solution (0.1 M PBS containing 5% goat serum and 0.3% Triton X-100). Appropriate Alexa Fluor dye-conjugated secondary antibodies (Invitrogen, Carlsbad, CA) were used at a dilution of 1:600 in 0.1 M PBS. Tissue sections were viewed and captured using a Spot Flex digital camera (Diagnostic Instruments, Inc. Sterling Heights, MI) attached to a Leica RX1500 upright microscope, and the images were collected using Spot software (Diagnostic Instruments, Inc.). The operator acquiring the images was blinded to group assignment.

Immunohistological image analysis

Histology sections were analyzed using ImagePro Plus software (Media Cybernetics, Inc.) using methods previously described (Sundberg et al., 2010). Briefly, percent areas of the histological markers were measured in a defined ROI using intensity thresholding. Randomly selected tissue sections from uninjured control animals were examined to determine normal levels of the fluorescent stain (Sundberg et al., 2010). ROIs were drawn in the ventral, lateral, and dorsal white matter in a similar manner to the DTI analysis, and the thresholds were applied.

Statistical analysis

Statistical analyses were performed using STATA (Intercooled Stata 9.2; StataCorp LP, College Station, TX). The Wilcoxon rank sum test was used for comparisons between groups at fixed time points as well as time-point comparisons within one group; Bonferroni correction was used for multiple comparisons where applicable. The Wilcoxon rank sum test was chosen for its robustness and lack of distribution

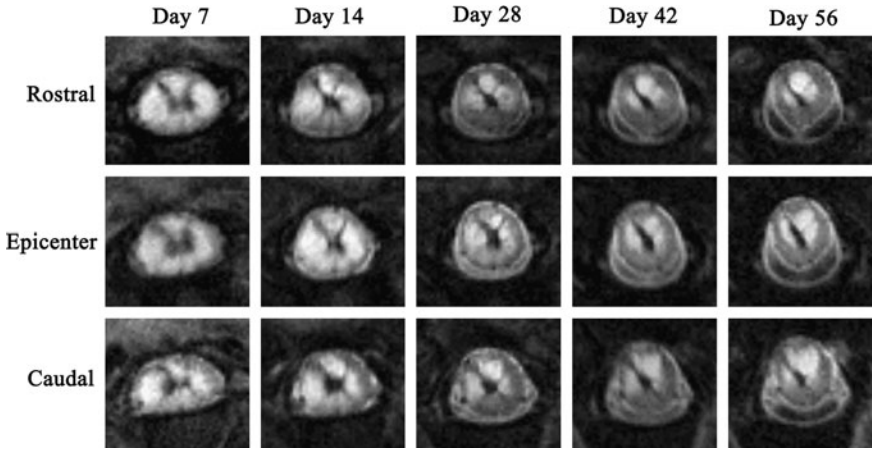

FIG. 1. Examples of magnetic resonance imaging (MRI) rapid acquisition by relaxation enhancement (RARE) images depicting lesion pathology in vehicle-treated spinal cord at each time point. Images at the epicenter and 1 mm rostral and caudal to the epicenter slice are shown.

restraints. Generalized estimating equation (GEE) analysis (Twisk and de Vente, 2002) was used to evaluate the temporal correlations within each group (Cohen et al., 2009), and Pearson's correlation analysis was used to evaluate relations between end-point histology and MRI and behavioral measures. All values are reported as mean ± standard deviation unless otherwise stated. Statistical significance was set at $p < 0.05$, with corrections for multiple comparisons (Bonferroni adjustment).

Results

MRI lesion volume

Figures 1 and 2 demonstrate changes in the hypo- and hyperintense lesion over time as seen in MRI RARE images of the vehicle-treated and VEGF-treated animals. In both groups the hyperintense lesion volume was largest at 7 days post-injury and subsequently decreased with time (Fig. 3A). However, there were no significant differences in lesion volumes between VEGF-treated and vehicle-treated animals at any time point. Inter-time-point comparisons were performed for each treatment group to evaluate the behavior of the lesion over time. Within the VEGF treatment group, there were significant differences between the hyperintense lesion volume at day 7 and chronic time points (days 28, 42, and 56; $p < 0.0018$). Vehicle-treated animals showed a similar significant decrease in lesion volume for acute time points (7 and 14 days) compared with chronic time points (days 28, 42, and 56; $p < 0.0059$). From day 28 onward, the hyperintense lesion volumes for VEGF-treated and vehicle-treated animals appeared to stabilize.

The VEGF-treated animals had significantly smaller hypointense lesion volumes compared to vehicle-treated animals ($p = 0.0026$) at days 14 and 28 post-SCI ($p = 0.0013$; Fig. 3B). The significant difference in hypointense lesion volume between VEGF-treated and vehicle-treated animals disappeared by 42 days post-SCI. Inter-time-point comparisons for each group indicated that the lesions remained relatively stable for the first 6 weeks of the study, with no significant differences between time points; however, at day 56 post-SCI

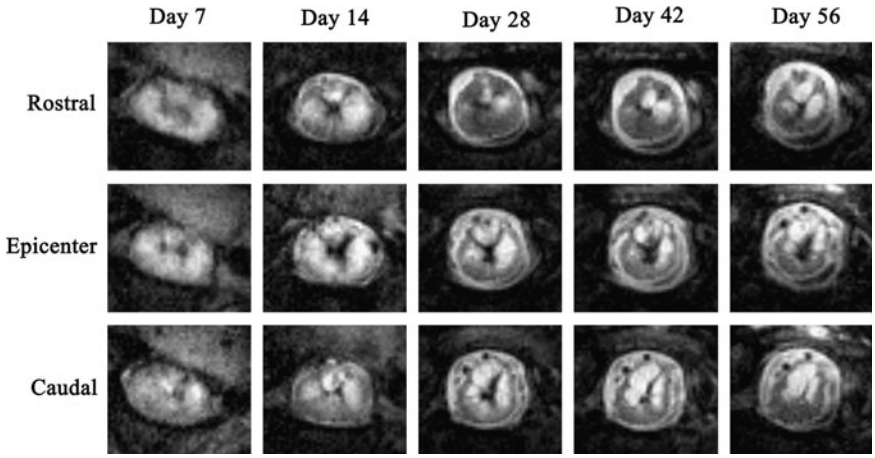

FIG. 2. Examples of magnetic resonance imaging (MRI) rapid acquisition by relaxation enhancement (RARE) images depicting lesion pathology in vascular endothelial growth factor (VEGF)-treated spinal cord at each time point. Images at the epicenter and 1 mm rostral and caudal to the epicenter slice are shown.

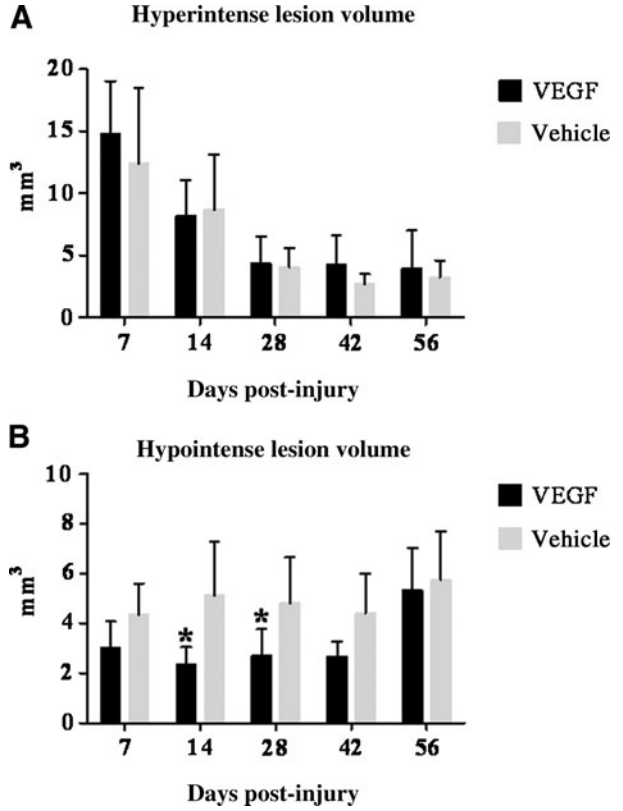

FIG. 3. Changes in the hyperintense and hypointense lesion volumes over the course of the 8-week study. (**A**) The hyperintense lesion is representative of edema and demyelination and indicated no significant differences between VEGF-treated and vehicle-treated animals at any time point. (**B**) The hypointense lesion, an indicator of hemorrhage and necrosis, indicated that the VEGF-treated animals had a significantly lower lesion volume at days 14 ($*p = 0.0017$) and 28 ($*p = 0.0001$). Error bars represent standard deviation (VEGF, vascular endothelial growth factor).

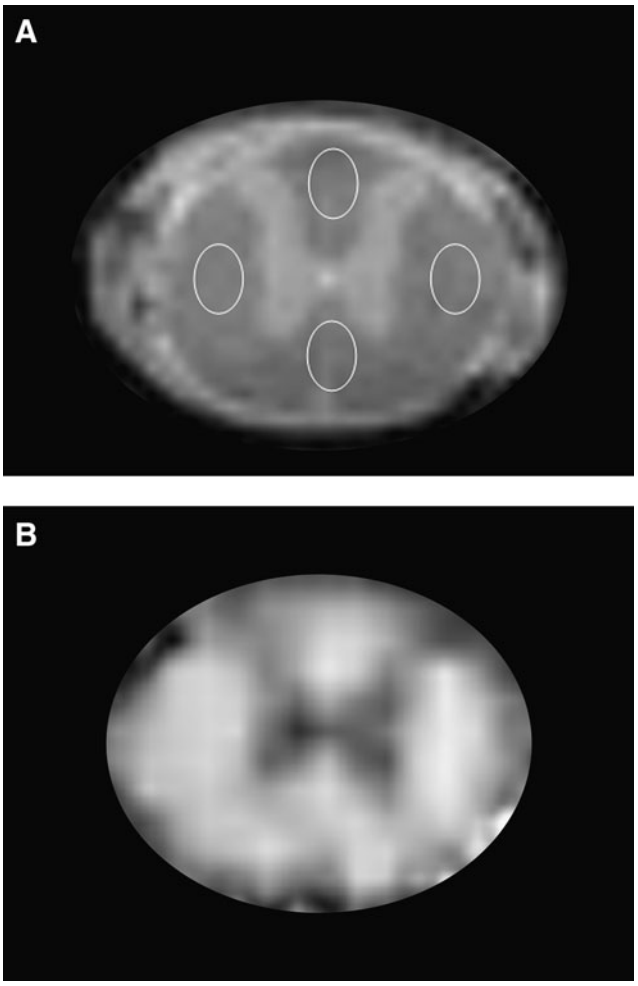

FIG. 4. (**A**) Locations of white matter regions of interest (ROIs), shown on an anatomical image of an uninjured spinal cord. For both diffusion tensor imaging (DTI) analysis and histological studies, similar ROIs were placed in the dorsal, lateral, and ventral white matter regions for comparison and correlation analysis. (**B**) Example of a fractional anisotropy (FA) map of an uninjured spinal cord. The hypointense region, indicative of low FA value, represents the gray matter.

the VEGF hypointense lesion volume increased and was significantly higher than at day 28 ($p = 0.0040$).

Diffusion tensor imaging after spinal cord injury

The DTI measures were evaluated in the slices that were rostral and caudal to the epicenter, and in three regions of white matter: dorsal, ventral, and lateral, as shown in Figure 4A. Similar ROIs were used for histological analyses so that DTI and histology could be compared. As an example, the FA map of an uninjured cord is shown in Figure 4B. As can be seen from this figure, the gray matter appears hypointense relative to the white matter because of its low diffusion anisotropy (Madi et al., 2005). Figures 5 and 6 show examples of FA maps derived from the DTI data in vehicle-treated and VEGF-treated animals taken from slices located in T5, T6, T8, and T9 at different time points. The epicenter region (T7) was not evaluated because of the complete loss of gray matter–white matter contrast. The hypointense lesions seen in these figures reflect lower FA that is typically observed in gray matter and disorganized tissues. As can be seen from these figures, the tissue architecture appears to be disrupted compared to the normal animal (Fig. 4B), even in regions that are away from the epicenter of injury. The values of the DTI measures showed similar patterns in all three white matter regions. The FA and λ_L values decreased with proximity to the injury epicenter, indicative of increased tissue disruption. Values for λ_T increased proximal to the epicenter, possibly indicating myelin disruption. All values of FA, λ_L, and λ_T throughout the spinal cord were significantly altered compared to uninjured values (Sundberg et al., 2010), signifying widespread damage to the white matter tracts.

Table 1 lists the observed significant differences by group and region. Significant changes in λ_L were observed at days 28 and 56. At day 28, λ_L values were decreased in the ventral ($p < 0.00001$) and lateral ($p < 0.00001$) white matter of VEGF-treated animals. At day 56 post-SCI, VEGF-treated animals had significantly lower λ_L values in the ventral ($p = 0.0011$) and dorsal ($p = 0.0027$) white matter regions. The VEGF-treated group had significantly lower dorsal λ_T values

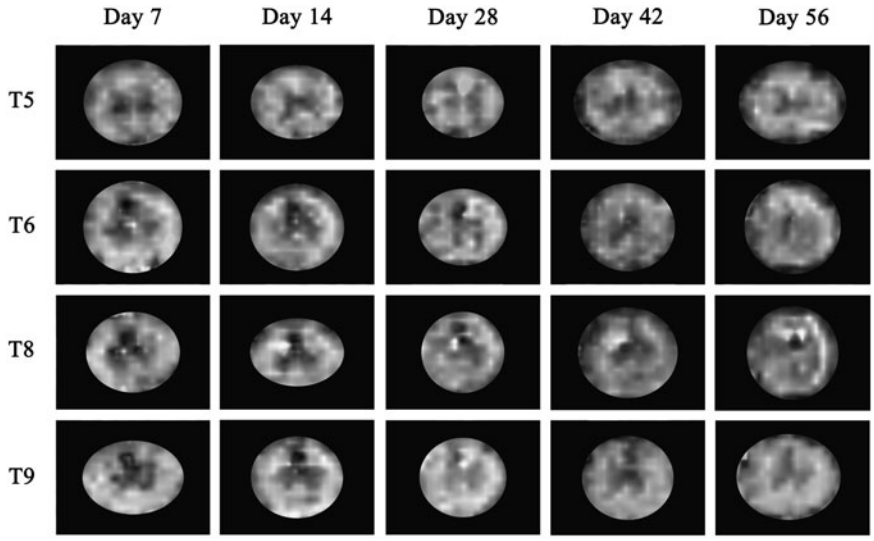

FIG. 5. Examples of fractional anisotropy (FA) maps derived from the diffusion tensor imaging (DTI) analysis of vehicle-treated animals at each time point. For DTI analysis all slices except the three epicenter slices, which corresponded to T7, were analyzed. The epicenter was excluded due to the complete loss of gray matter–white matter contrast. These images show examples of slices taken from T5, T6, T8, and T9. The hypointense regions indicate lower FA values. Note that gray matter structures have lower FA values than the white matter regions.

compared with vehicle-treated animals ($p = 0.0019$) at day 14. The VEGF-treated group also had significantly lower λ_T values in the ventral white matter on day 28 ($p < 0.00001$), and in the lateral ($p < 0.00001$) and dorsal ($p = 0.0001$) white matter at day 56. There were no significant differences between FA values for any region at any of the reported time points.

Neurobehavioral and sensory assays

The Basso, Beattie, and Bresnahan (BBB) open-field locomotor test was performed at post-injury days 3, 7, 14, 28, 42, and 56. The results for the BBB test, inclined plane test, and grid walk test are listed in Table 2. All animals showed a severely diminished BBB score immediately after SCI, followed by an improvement in performance over time. VEGF-treated animals had an average BBB score of 1.3 ± 1.68 on day 3 and vehicle-treated animals had a score of 0.7 ± 0.82, while maximum scores of 13.9 ± 2.19 and 14.6 ± 2.76 were recorded on day 56. Both groups performed similarly and there were no significant differences at any time point.

Additional neurobehavioral assays were incorporated once the animals demonstrated weight support. On day 14 the VEGF-treated animals could maintain their balance at an angle of $44.1 \pm 5.45°$ and vehicle-treated animals at an angle of

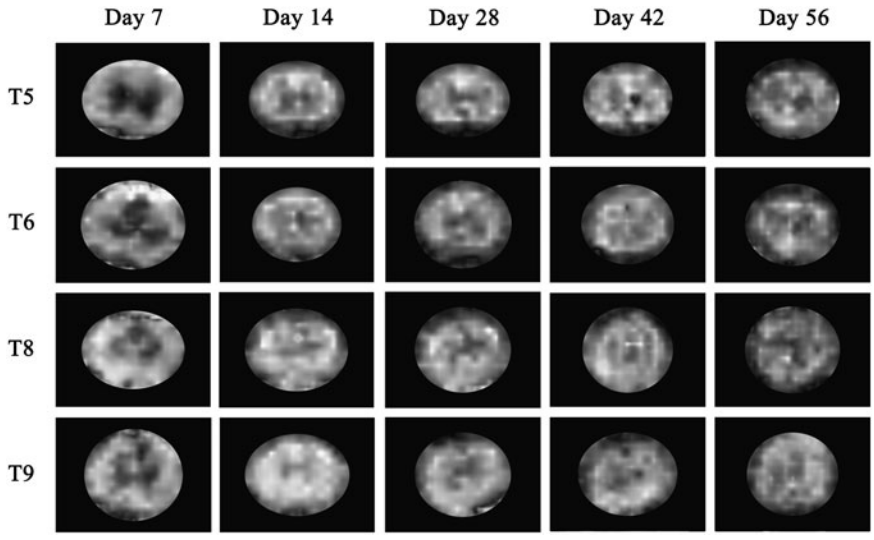

FIG. 6. Examples of diffusion tensor imaging (DTI) images in vascular endothelial growth factor (VEGF)-treated animals at each time point. For DTI analysis, all slices except for the three epicenter slices, which corresponded to T7, were analyzed. The epicenter was excluded due to the complete loss of gray matter–white matter contrast. These images show examples of slices taken from T5, T6, T8, and T9.

Table 1. DTI Measures for All Regions and Time Points for which Significant Differences Were Observed

Measure	*Time point*	*VEGF*	*Vehicle*	p *Value*
λ_T Dorsal	Day 14	0.35 ± 0.152	0.52 ± 0.248	0.0019
λ_T Ventral	Day 28	0.40 ± 0.111	0.46 ± 0.129	< 0.00001
λ_L Ventral	Day 28	1.16 ± 0.233	1.26 ± 0.200	< 0.00001
λ_L Lateral	Day 28	1.04 ± 0.180	1.15 ± 0.191	< 0.00001
λ_T Lateral	Day 56	0.44 ± 0.195	0.48 ± 0.199	< 0.00001
λ_T Dorsal	Day 56	0.58 ± 0.438	0.63 ± 0.334	0.0001
λ_L Ventral	Day 56	1.25 ± 0.254	1.21 ± 0.254	0.0011
λ_L Dorsal	Day 56	1.23 ± 0.428	1.32 ± 0.343	0.0027

Values are expressed as the group mean ± standard deviation.
λ_L, longitudinal diffusivity; λ_T, transverse diffusivity; DTI, diffusion tensor imaging; VEGF, vascular endothelial growth factor.

44.7 ± 6.20°. By day 56 the VEGF-treated and vehicle-treated groups remained on the plane at angles of 49.9 ± 3.23°and 51.6 ± 2.57°, respectively. There were no significant differences between the two groups throughout the course of the study.

Similarly to the results seen with the BBB and inclined plane tests, all animals showed some improvement in their performance on the grid walk over time. At day 14, VEGF-treated animals had 16.8 ± 4.07 footfaults, and vehicle-treated animals had 12.0 ± 5.45. By day 56 the VEGF-treated group improved to 8.2 ± 5.73 footfaults and vehicle-treated animals to 8.0 ± 4.69 hindlimb footfaults. There were no significant differences at any time point.

Animals underwent assessment for allodynia using the von Frey Filament test. Using the approach previously described (Nesic-Taylor et al., 2010; Sundberg et al., 2010) for quantifying pain and persistent allodynia, we observed that 33.3% of VEGF-treated rats expressed persistent allodynia, while significantly fewer of the vehicle-treated animals (7.7%; $p < 0.05$) had chronic allodynia.

The animals were also tested in the computerized activity box to assess rearing and exploratory behaviors at post-injury days 14, 28, 42, and 56. The results indicated no significant differences in rearing or exploratory behavior at any of the examined time points.

Histological analysis between treatment groups

Immunofluorescence labeling was performed to correlate with DTI measures. Examples of representative immunofluorescence images of neurofilament and oligodendrocyte/myelin labels in the dorsal columns are shown in Figures 7 and 8, respectively. Quantitative results for immunolabeling are also shown in Figures 7 and 8.

The quantitative results for neurofilament indicated that there were no significant differences between the VEGF-treated and vehicle-treated animals at day 56 (Fig. 7).

The antibody labeling for oligodendrocytes/myelin indicated a significant increase in the percentage labeling in the dorsal ($p < 0.00001$), lateral ($p = 0.0168$), and ventral ($p = 0.0073$) white matter of VEGF-treated animals compared to vehicle-treated animals in these white matter columns (Fig. 8).

Correlations with MRI measures

Results of the GEE analysis of DTI data are summarized in Tables 3 and 4. In the rostral region, VEGF treatment resulted in significant correlations between the dorsal white matter FA values and BBB scores ($p = 0.010$; Table 3). In this same region, the grid walk performance significantly correlated with λ_L ($p = 0.003$) and λ_T ($p = 0.004$) measures. In the ventral ROI located in the rostral region, performance on the grid walk test also significantly correlated with λ_T ($p = 0.003$).

In the caudal region there were only a few significant correlations between DTI measures and behavioral data (Table 4). In the dorsal white matter of VEGF-treated animals there were significant correlations between λ_L and inclined plane ($p = 0.010$), and λ_T and rearing ($p = 0.001$). In the lateral white matter there were no correlations between DTI and behavior for both VEGF-treated and vehicle-treated animals. In the ventral region there were no significant correlations within the VEGF group, and grid walk correlated with both FA and λ_T for the vehicle-treated animals.

Table 2. Performance of VEGF-Treated and Vehicle-Treated Animals on Neurobehavioral Testing

	BBB		*Inclined plane*		*Grid walk*	
	VEGF	*Vehicle*	*VEGF*	*Vehicle*	*VEGF*	*Vehicle*
Day 3	1.3 ± 1.68	0.7 ± 0.82				
Day 7	6.3 ± 2.56	7.1 ± 2.21				
Day 14	10.6 ± 2.06	10.8 ± 2.93	44.1 ± 5.45	44.7 ± 6.20°	16.8 ± 4.07	12.0 ± 5.45
Day 28	13.1 ± 2.13	13.1 ± 2.70	48.9 ± 4.36°	48.4 ± 4.37°	11.0 ± 3.59	12.4 ± 6.20
Day 42	13.5 ± 1.95	14.1 ± 2.79	48.1 ± 4.26	49.3 ± 3.02°	9.9 ± 4.68	9.4 ± 4.38
Day 56	13.9 ± 2.19	14.6 ± 2.76	49.9 ± 3.23	51.6 ± 2.57°	8.2 ± 5.73	8.0 ± 4.69

BBB performance was assessed at all time points following surgery; inclined plane was incorporated once animals could maintain a weight-supported stance; grid walk was added once animals could take weight-supported steps. There were no significant differences for all behavioral assays. All values are expressed as group mean ± standard deviation.
BBB, Basso, Beattie, and Bresnahan rating scale; VEGF, vascular endothelial growth factor.

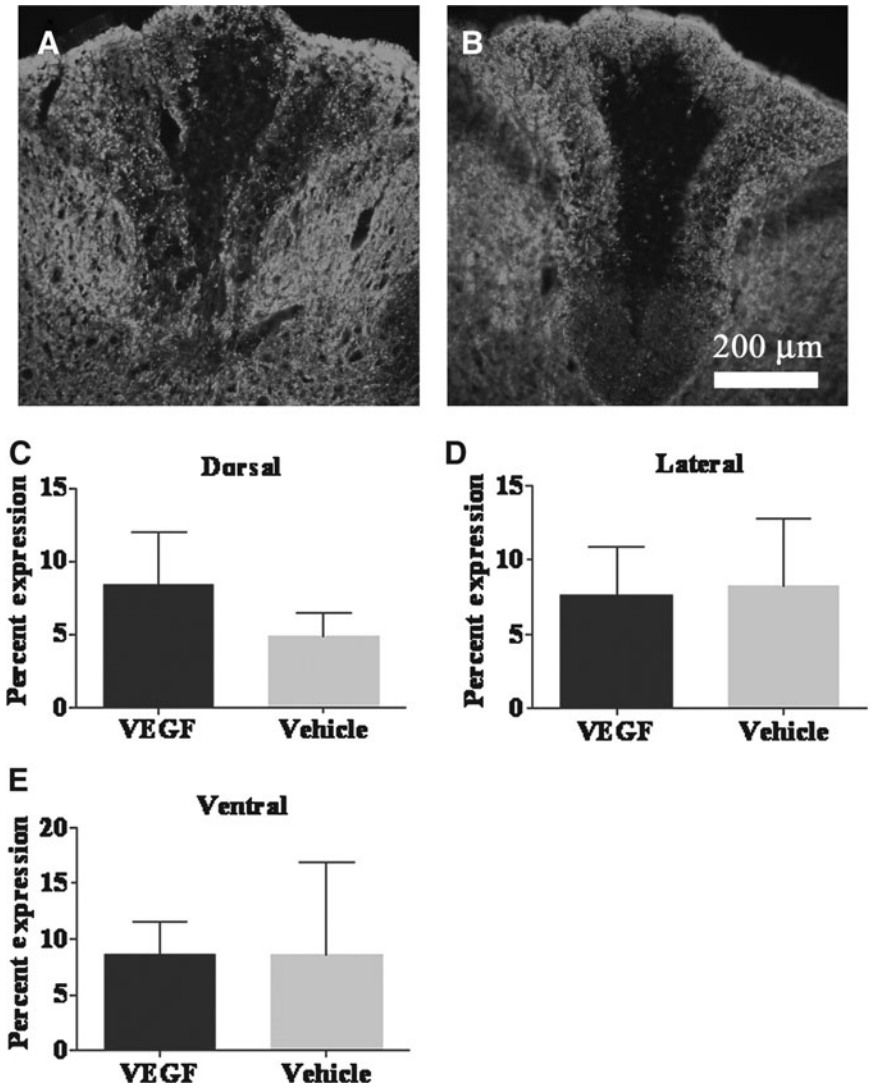

FIG. 7. Representative images of the spinal cord dorsal columns in fluorescently-stained vascular endothelial growth factor (VEGF)-treated (**A**) and vehicle-treated (**B**) tissues at 20× magnification. The tissues were stained with the neurofilament protein SMI-31R. At post-injury day 56, quantitative analysis of the percentage expression of neurofilament showed no significant difference in labeling in the dorsal (**C**), lateral (**D**), or ventral (**E**) columns of VEGF-treated animals compared to vehicle-treated animals.

The results of the GEE analysis of lesion volume are summarized in Table 5. In the VEGF-treated animals there were significant correlations between the hyperintense lesion volume and performance on the BBB assay ($p < 0.0001$), grid walk ($p < 0.0001$), and rearing ($p < 0.0001$). In the vehicle-treated animals there was only a single correlation, between hyperintense lesion volume and the grid walk test. The hypointense lesion correlated only with performance on the grid walk assay in VEGF-treated animals ($p < 0.0001$). There were no correlations between hypointense lesion volume in the vehicle-treated animals and behavioral measures.

Since histological data were collected only at day 56, the GEE analysis could not performed to examine possible correlations between histology and DTI and neurobehavioral measures. Instead, we used Pearson's correlation to compare the end-point histology to neurobehavioral and DTI data for day 56 only. There were no significant correlations found for any regional histology measures and behavioral assays in the VEGF-treated animals.

Discussion

Acute treatment with VEGF results in tissue sparing

The results from our study indicate that at days 14 and 28 VEGF-treated animals had significantly less tissue necrosis than vehicle-treated animals, as determined by the reduction in the hypointense lesion volumes seen on MRI. Previous studies have determined that the initial hemorrhage following injury begins to resolve within the first week (Beattie et al., 2002; Noble and Wrathall, 1987; Profyris et al., 2004); therefore, the hypointense lesion seen at later time points mainly reflects tissue necrosis (Weirich et al., 1990). The observed reduction in hypointense lesion volume may be attributed to the neuroprotective effect of VEGF, resulting in tissue sparing, and/or its ability to stimulate proliferation of neurons and axonal sprouting (Brockington et al., 2004; Sondell et al., 1999, 2000). The hypointense lesion volume seen in the VEGF-treated animals was not significantly different from vehicle-

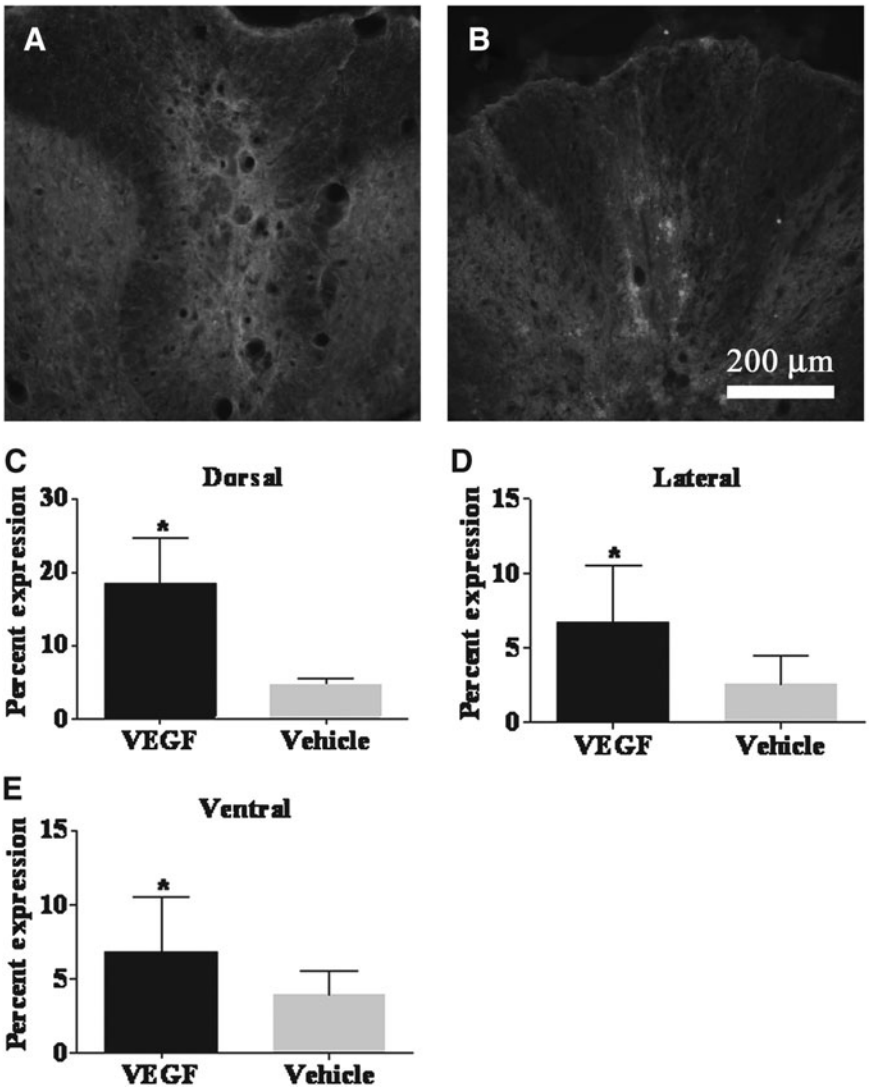

FIG. 8. Representative images of the spinal cord dorsal columns in fluorescently-stained vascular endothelial growth factor (VEGF)-treated (**A**) and vehicle-treated (**B**) tissues at 20× magnification. The tissues were stained with MAB 328 for oligodendrocytes/myelin. Quantitative analysis of the percentage expression of the labeling of oligodendrocytes/myelin was significantly increased in the (**C**) dorsal columns of VEGF-treated animals compared to vehicle-treated animals ($*p < 0.00001$). The percentage expression was also significantly increased in the (**D**) lateral region ($*p = 0.0168$) and (**E**) ventral region ($*p = 0.0073$) of VEGF-treated animals compared to vehicle-treated animals.

treated animals at post-injury days 42 and 56. This suggests that the beneficial effects of a single acute injection of VEGF were not sustained. Furthermore, intra-group comparisons indicated that the hypointense lesion volume in VEGF-treated animals significantly increased in volume between days 28 and 56 ($p = 0.0040$). It is well known that the secondary injury continues to spread well into the chronic phase of injury (Hagg and Oudega, 2006). It is possible that delivery of VEGF in the acute phase of SCI delays the spread of injury due to its neuroprotective effects, but these effects are not maintained and eventually the secondary injury processes rebound and exacerbate the injury. It is possible that multiple treatments with VEGF may help sustain the improvement.

Histological measures were performed only at the conclusion of the MRI experiments on day 56. The MRI data for that time point indicated that there were no significant differences in the total hypointense lesion volume between the two groups of animals. Consistent with these findings, the histological labeling for neurofilament showed no significant differences between the VEGF-treated and vehicle-treated groups in any region. At earlier time points where MRI showed significantly smaller hypointense lesions in the VEGF-treated group, we speculate that we would have observed a significant increase in positive neurofilament staining to indicate spared tissue or neurogenesis; however, that has yet to be confirmed.

Acute delivery of VEGF does not significantly alter the volume of the hyperintense lesion

The MRI hyperintense lesion reflects edema in the early stages of injury (Weirich et al., 1990). Studies in cats and monkeys have shown that edema occurs within 30 sec of injury and becomes prominent within 5 min (Demediuk et al.,

Table 3. Correlations between DTI Measures from the Rostral Region of the Spinal Cord and Neurobehavioral Assays

	Rostral region			
	VEGF		*Vehicle*	
Dorsal	FA -BBB	$p=0.010$	λ_L - BBB	$p=0.004$
	λ_L - GW	$p=0.003$	λ_T - IP	$p=0.002$
	λ_T - GW	$p=0.004$		
Lateral			FA - IP	$p<0.0001$
			FA - rearing	$p<0.0001$
			λ_L - BBB	$p=0.008$
			λ_T - GW	$p=0.001$
			λ_T - IP	$p=0.001$
Ventral	λ_T - GW	$p=0.003$	FA - BBB	$p=0.008$
			FA - IP	$p=0.010$
			FA - Rearing	$p<0.0001$
			λ_T - BBB	$p=0.001$
			λ_T - IP	$p=0.009$
			λ_T - Rearing	$p=0.001$

Generalized estimating equation (GEE) analysis was used to correlate behavioral assay data with DTI measures in the dorsal, lateral, and ventral white matter areas.

BBB, Basso, Beattie, and Bresnahan test; IP, inclined plane test, GW, grid walk test; FA, fractional anisotropy; λ_L, longitudinal diffusivity; λ_T, transverse diffusivity; DTI, diffusion tensor imaging; VEGF, vascular endothelial growth factor.

1987; Nolan, 1969; Sharma, 2005; Yashon et al., 1973). Edema has been shown to start to regress by 9 days post-SCI in cats (Reulen, 1976, 1977; Sharma, 2005). However, in humans significant edema has been observed to persist for weeks following injury (Goldsmith, 1999).

In our study, the hyperintense lesion was largest on day 7 and decreased with time. There were no significant differences in the hyperintense lesion volume between the VEGF-treated and vehicle-treated animals at any time point. Because contusive SCI elicits an overwhelming response within the tissue and causes massive disruption of the vasculature and production of edema, it is possible that the treatments had little measurable impact on the overall volume of edema at the early time points. Alternatively, VEGF may actually increase edema due to its permeabilizing effect on the vasculature, but

Table 4. Correlations between DTI Measures from the Caudal Region of the Spinal Cord and Neurobehavioral Assays

	Caudal region			
	VEGF		*Vehicle*	
Dorsal	λ_L - IP	$p=0.010$		
	λ_T - rearing	$p=0.001$		
Ventral			FA - GW	$p=0.007$
			λ_T - GW	$p=0.005$

Generalized estimating equation (GEE) analysis was used to correlate behavioral assay data with DTI measures in the dorsal, lateral, and ventral white matter areas.

IP, inclined plane test, GW, grid walk test; FA, fractional anisotropy; λ_L, longitudinal diffusivity; λ_T, transverse diffusivity; DTI, diffusion tensor imaging; VEGF, vascular endothelial growth factor.

Table 5. Correlations between Lesion Volume and Neurobehavioral Assays

	VEGF				
	BBB	*GW*	*IP*	*VF*	*Rearing*
Hypointense volume		$p<0.0001$			
Hyperintense volume	$p<0.0001$	$p<0.0001$			$p<0.0001$
	Vehicle				
	BBB	*GW*	*IP*	*VF*	*Rearing*
Hypointense volume					
Hyperintense volume		$p=0.006$			

Generalized estimating equation (GEE) analysis was used to correlate the longitudinal hypointense and hyperintense lesion volume values from each treatment group with behavioral assay data.

BBB, Basso, Beattie, and Bresnahan test; IP, inclined plane test, GW, grid walk test; VEGF, vascular endothelial growth factor; VF, von Frey filament test.

may spare the myelin. Edema and myelin have opposing effects on hyperintense lesions (Weirich et al., 1990), therefore there may not be any detectable change in the hyperintense lesion volume. While no histology was performed at time points before 56 days post-SCI to confirm this possibility, the histological stains indicated that VEGF-treated animals had significantly increased markers for myelin and oligodendrocytes at day 56.

Though there were no differences between the groups at individual time points, comparisons of lesion volume within each group indicated that the hyperintense lesion in both the VEGF-treated and vehicle-treated animals significantly decreased between early and chronic time points, and that a plateau was reached by day 28. This suggests that at post-injury day 28 the edema had resolved, and any remaining hyperintense lesion could be attributed to demyelination.

VEGF treatment may result in oligodendrogenesis

Immunohistochemical analyses using a marker that binds to both myelin and oligodendrocytes showed a significant increase in labeling in the VEGF-treated animals compared to the vehicle-treated animals. It is possible that acute treatment with VEGF may actually result in an increased number of oligodendrocyte progenitors. A recent study by Kim and associates (2009), found that transplantation of F3.VEGF cells, which are immortalized human NSC cells that are retrovirally transduced to overexpress VEGF, following SCI significantly increased the number of $NG2^+$ glial progenitor cells 2 weeks after injury, and that these proliferating progenitor cells differentiated into oligodendrocytes by 6 weeks post-injury (Kim et al., 2009). The authors concluded that the increased number of glial progenitor cells and oligodendrocytes could stimulate remyelination and lead to improved functional recovery. Alternatively, the increased fluorescent staining of the myelin and oligodendrocyte marker in the VEGF-treated animals compared to vehicle controls may indicate enhanced sparing of white matter, as observed in a previous VEGF study (Widenfalk et al., 2003).

In the current studies we did not observe significant differences in the performance of VEGF-treated versus vehicle-

treated animals for any of the behavioral tests. However, improvements in neurobehavioral outcome may potentially occur at a time point later than 56 days post-SCI.

Effects of acute VEGF treatment on white matter fiber tract integrity

The DTI data provided information on the state of axonal and myelin integrity. No significant differences between measures of FA for the VEGF-treated and vehicle control groups were found. FA is a measure of the overall anisotropy of water molecules within the tissue, and provides a general indicator of the state of the white matter; however, FA does not provide specific information about underlying tissue pathology. The measures of λ_L and λ_T provide more specific information about axonal loss and myelin integrity (Budde et al., 2009; Deo et al., 2006; Herrera et al., 2009; Song et al., 2002, 2005).

In these studies, significant differences in λ_L and λ_T values were found for the VEGF and vehicle animals at several time points. It was observed that at days 28 and 56 post-injury, the λ_L values in VEGF-treated animals were decreased compared to those in vehicle-treated animals. Previous studies have found correlations between λ_L and axonal integrity (Budde et al., 2007, 2009; DeBoy et al., 2007; Kozlowski et al., 2008; Song et al., 2002, 2005), therefore these results suggest that treatment of SCI with VEGF leads to further disruption of the white matter tracts. However, end-point histology showed no significant differences between the two groups in the percentage expression of phosphorylated neurofilament present within the tissue. We previously reported that it is possible that SCI affects the DTI measures in a complex manner, so that the λ_L values are not solely attributable to neuronal integrity (Sundberg et al., 2010). For example, the λ_L values may also be affected by the caliber of the axons (Harsan et al., 2006). It is therefore possible that VEGF treatment resulted in a reduction in axonal caliber, rather than axonal loss, which resulted in lower λ_L values. Alternatively, VEGF is known to promote axonal outgrowth and thus may induce random axonal sprouting, which reduces axonal coherence.

It was also observed that λ_T was significantly decreased in VEGF-treated animals compared to vehicle-treated animals as early as 14 days post-SCI. This suggests that the VEGF-treated animals have improved myelin integrity compared to the vehicle-treated animals. Histological analysis showed that VEGF-treated animals had significantly increased levels of myelin and oligodendrocytes at day 56. It is possible that VEGF treatment resulted in better preservation of myelin following SCI, as intact myelin sheaths help to constrain the diffusion of water within the fiber tracts, and result in decreased λ_T values. Alternatively, as mentioned in reference to the hyperintense lesion, it is possible that the VEGF-treated animals had increased numbers of oligodendrocytes rather than spared myelin. The increased presence of oligodendrocytes in the VEGF-treated spinal cords, which occupy the spaces left by the reduced-caliber axons, may also result in decreased λ_T values, and suggest the potential for future remyelination.

Acute VEGF treatment of SCI does not affect functional outcome and may lead to chronic allodynia

In these studies, no differences were observed for the neurobehavioral tests of functional recovery within the 56-day time period. It is possible that VEGF treatment may elicit significant changes in outcome at later time points; however, this has yet to be confirmed. The increased numbers of oligodendrocytes seen within the VEGF-treated spinal cords potentially indicate that remyelination may occur, and lead to an eventual improvement in functional outcome.

We chose to incorporate the von Frey test for mechanical allodynia in these studies, as many SCI patients develop chronic pain (Dijkers et al., 2009). While there were no observable differences between the two groups in performance on sensorimotor tasks, significant differences in outcome emerged in the von Frey filament test for mechanical allodynia. It was observed that a small subset of vehicle-treated animals developed chronic allodynia after SCI; however, significantly more VEGF-treated animals exhibited allodynia. Taking into account the increased volume in spared tissue as determined by MRI, coupled with the potential for remyelination, it is possible that VEGF treatment may play a role in promoting plasticity in sensory pathways that may lead to chronic pain conditions. The potential mechanisms underlying this phenomenon were further explored by Nesic and colleagues (Nesic-Taylor et al., 2010).

After completion of this article, a study examined the repeated intrathecal administration of VEGF after injury, beginning 24 h after injury and lasting for 7 days. The results from that study indicated that using that particular route of administration resulted in a significant decrease in mechanical allodynia with hindpaw stimulation (van Neerven et al., 2010). Our own study indicated that there was a significant increase in forepaw hypersensitivity of VEGF-treated animals (Nesic-Taylor et al., 2010). The differences in these results may be attributable to the routes of administration, and should be considered in future SCI studies using VEGF.

Correlations between MRI measures and neurobehavioral assays

Correlation analysis between DTI measures, neurobehavioral outcome, and histology provided mixed results. Several issues likely affected the ability to determine consistent correlations between DTI measures, histology, and neurobehavioral performance. One issue is that the behavioral assays involve the coordination of multiple spinal cord tracts that are not exclusively located in one region of white matter; therefore a direct correlation may not exist with DTI or histology measures from a single white matter region (ventral, lateral, or dorsal). Additionally, a single ROI may actually encompass more than one white matter tract, and may result in a loss of correlation with the behavioral assay.

Comparisons between hyperintense and hypointense lesion volumes and performance on neurobehavioral assays also provided mixed results for the treatment groups. The VEGF-treated group had longitudinal correlations between the hyperintense lesion and performance on the BBB and grid walk assays, as well as with the number of rearing events; vehicle-treated animals only showed significant correlations between hyperintense lesion volume and grid walk performance. There were no significant differences in performance between the injured groups on these assays, and all animals improved over time, while showing a simultaneous reduction

in hyperintense lesion volume. Studies have shown that edema can remain in the tissue for over 2 weeks after SCI (Demediuk et al., 1987; Mihai et al., 2008; Nolan, 1969; Sharma, 2005), and it is known that a relationship between edema and cord swelling exists (Mihai et al., 2008). The improved performance on behavioral tasks in our study was likely due to a reduction in spinal cord swelling and pressure on the fiber tracts. However, MRI hyperintensity is also known to reflect demyelination, and therefore remyelination would have the opposite effect on hyperintense lesions. As remyelination occurs, the hyperintense lesion volume could decrease and result in improved performance on behavior tasks. While there are no histological data providing information about the degree of myelination within the tissue at early time points, the data suggest the presence of oligodendrocytes at day 56.

In the vehicle-treated animals the hypointense lesion volume did not correlate with neurobehavioral outcomes; however, VEGF-treated animals showed a correlation between the hypointense lesion and performance on the grid walk test. VEGF-treated animals had increased tissue sparing at certain time points compared to the vehicle-treated animals, and therefore this correlation may relate to better maintenance of spinal cord tracts involved in the grid walk task.

Conclusions

Previous studies have provided conflicting information regarding the therapeutic benefits of $VEGF_{165}$ treatment following SCI. The discrepancies in the results may be attributed to a number of factors, that include differences in injury protocols, the type and/or severity of injury, dosage, method of delivery, timing of delivery, and duration of treatment. Based on the results from this study, acute administration of $VEGF_{165}$ after SCI appears to attenuate cavity formation, results in tissue sparing, and may result in oligodendrogenesis. $VEGF_{165}$ may increase perfusion and help to promote an environment that is permissive to axonal regrowth. However, $VEGF_{165}$ treatment may also play a role in promoting plasticity following SCI, which may lead to chronic pain conditions.

Author Disclosure Statement

No competing financial interests exist.

References

Basso, D.M., Beattie, M.S. ,and Bresnahan, J.C. (1995). A sensitive and reliable locomotor rating scale for open field testing in rats. J. Neurotrauma 12, 1–21.

Beattie, M.S., Hermann, G.E., Rogers, R.C., and Bresnahan, J.C. (2002). Cell death in models of spinal cord injury. Prog. Brain Res. 137, 37–47.

Benton, R.L., and Whittemore, S.R. (2003). VEGF165 therapy exacerbates secondary damage following spinal cord injury. Neurochem. Res. 28, 1693–1703.

Bockhorst, K.H., Hui, C.K., and Narayana, P.A. (2010a). Fully automatic postprocessing and evaluation of DTI Data: Unsupervised pipeline for batch jobs, in: 18th Annual Meeting of the International Society for Magnetic Resonance in Medicine. Stockholm, Sweden.

Bockhorst, K.H., Narayana, P.A., Dulin, J., Liu, R., Rea, H.C., Hahn, K., Wosik, J., and Perez-Polo, J.R. (2010b). Normobaric hyperoximia increases hypoxia-induced cerebral injury: DTI study in rats. J. Neurosci. Res. 88, 1146–1156.

Bockhorst, K.H., Narayana, P.A., Liu, R., Ahobila-Vijjula, P., Ramu, J., Kamel, M., Wosik, J., Bockhorst, T., Hahn, K., Hasan, K.M., and Perez-Polo, J.R. (2008). Early postnatal development of rat brain: in vivo diffusion tensor imaging. J. Neurosci. Res. 86, 1520–1528.

Bresnahan, J.C., Beattie, M.S., Todd, F.D., 3rd, and Noyes, D.H. (1987). A behavioral and anatomical analysis of spinal cord injury produced by a feedback-controlled impaction device. Exp. Neurol. 95, 548–570.

Brockington, A., Lewis, C., Wharton, S., and Shaw, P.J. (2004). Vascular endothelial growth factor and the nervous system. Neuropathol. Appl. Neurobiol. 30, 427–446.

Budde, M.D., Kim, J.H., Liang, H.F., Schmidt, R.E., Russell, J.H., Cross, A.H., and Song, S.K. (2007). Toward accurate diagnosis of white matter pathology using diffusion tensor imaging. Magn. Reson. Med. 57, 688–695.

Budde, M.D., Xie, M., Cross, A.H., and Song, S.K. (2009). Axial diffusivity is the primary correlate of axonal injury in the experimental autoimmune encephalomyelitis spinal cord: a quantitative pixelwise analysis. J. Neurosci. 29, 2805–2813.

Cohen, D.M., Patel, C.B., Ahobila-Vajjula, P., Sundberg, L.M., Chacko, T., Liu, S.J., and Narayana, P.A. (2009). Blood-spinal cord barrier permeability in experimental spinal cord injury: dynamic contrast-enhanced MRI. NMR Biomed. 22, 332–341.

DeBoy, C.A., Zhang, J., Dike, S., Shats, I., Jones, M., Reich, D.S., Mori, S., Nguyen, T., Rothstein, B., Miller, R.H., Griffin, J.T., Kerr, D.A., and Calabresi, P.A. (2007). High resolution diffusion tensor imaging of axonal damage in focal inflammatory and demyelinating lesions in rat spinal cord. Brain 130, 2199–2210.

Demediuk, P., Saunders, R.D., Anderson, D.K., Means, E.D., and Horrocks, L.A. (1987). Early membrane lipid changes in laminectomized and traumatized cat spinal cord. Neurochem. Pathol. 7, 79–89.

Deo, A.A., Grill, R.J., Hasan, K.M., and Narayana, P.A. (2006). In vivo serial diffusion tensor imaging of experimental spinal cord injury. J. Neurosci. Res. 83, 801–810.

Dijkers, M., Bryce, T., and Zanca, J. (2009). Prevalence of chronic pain after traumatic spinal cord injury: a systematic review. J. Rehabil. Res. Dev. 46, 13–29.

Facchiano, F., Fernandez, E., Mancarella, S., Maira, G., Miscusi, M., D'Arcangelo, D., Cimino-Reale, G., Falchetti, M.L., Capogrossi, M.C., and Pallini, R. (2002). Promotion of regeneration of corticospinal tract axons in rats with recombinant vascular endothelial growth factor alone and combined with adenovirus coding for this factor. J. Neurosurg. 97, 161–168.

Fenyes, D.A., and Narayana, P.A. (1998). In vivo echo-planar imaging of rat spinal cord. Magn. Reson. Imaging 16, 1249–1255.

Ferrara, N., Gerber, H.P., and LeCouter, J. (2003). The biology of VEGF and its receptors. Nat. Med. 9, 669–676.

Goldsmith, H.S. (1999). Acute spinal cord injuries: a search for functional improvement. Surg. Neurol. 51, 231–233.

Hagg, T., and Oudega, M. (2006). Degenerative and spontaneous regenerative processes after spinal cord injury. J. Neurotrauma 23, 264–280.

Hahn, K., Prigarin, S., and Hasan, K. (2004). A novel denoising technique for very noisy DTI data, in: The International Society for Magnetic Resonance in Medicine. Kyoto, Japan, p. 1208.

Hahn, K., Prigarin, S., and Hasan, K. (2005). The feasibility of diffusion tensor imaging for the human brain at 1 mm^3 reso-

lution, in: The International Society for Magnetic Resonance in Medicine. Miami, Florida, p. 161.

Harsan, L.A., Poulet, P., Guignard, B., Steibel, J., Parizel, N., de Sousa, P.L., Boehm, N., Grucker, D., and Ghandour, M.S. (2006). Brain dysmyelination and recovery assessment by noninvasive in vivo diffusion tensor magnetic resonance imaging. J. Neurosci. Res. 83, 392–402.

Herrera, J.J., Nesic-Taylor, D.O., and Narayana, P.A. (2009). Reduced vascular endothelial growth factor expression in contusive spinal cord injury. J Neurotrauma 26, 995–1003.

Jiang, H., van Zijl, P.C., Kim, J., Pearlson, G.D., and Mori, S. (2006). DtiStudio: resource program for diffusion tensor computation and fiber bundle tracking. Comput. Methods Programs Biomed. 81, 106–116.

Kim, H.M., Hwang, D.H., Lee, J.E., Kim, S.U., and Kim, B.G. (2009). Ex vivo VEGF delivery by neural stem cells enhances proliferation of glial progenitors, angiogenesis, and tissue sparing after spinal cord injury. PLoS One. 4, e4987.

Kozlowski, P., Raj, D., Liu, J., Lam, C., Yung, A.C., and Tetzlaff, W. (2008). Characterizing white matter damage in rat spinal cord with quantitative MRI and histology. J. Neurotrauma 25, 653–676.

Madi, S., Hasan, K.M., and Narayana, P.A. (2005). Diffusion tensor imaging of in vivo and excised rat spinal cord at 7 T with an icosahedral encoding scheme. Magn. Reson. Med. 53, 118–125.

Mihai, G., Nout, Y.S., Tovar, C.A., Miller, B.A., Schmalbrock, P., Bresnahan, J.C., and Beattie, M.S. (2008). Longitudinal comparison of two severities of unilateral cervical spinal cord injury using magnetic resonance imaging in rats. J. Neurotrauma 25, 1–18.

Mills, C.D., Grady, J.J., and Hulsebosch, C.E. (2001). Changes in exploratory behavior as a measure of chronic central pain following spinal cord injury. J. Neurotrauma 18, 1091–1105.

Nesic-Taylor, D.O., Sundberg, L.M., Herrera, J.J., Mokkapati, V.U., Lee, J., and Narayana, P.A. (2010). VEGF and spinal cord injury pain. J. Neurotrauma 27, 1793–1803.

Noble, L.J., and Wrathall, J.R. (1987). The blood-spinal cord barrier after injury: pattern of vascular events proximal and distal to a transection in the rat. Brain Res. 424, 177–188.

Nolan, R.T. (1969). Traumatic oedema of the spinal cord. Br. Med. J. 1, 710.

Otrock, Z.K., Mahfouz, R.A., Makarem, J.A., and Shamseddine, A.I. (2007). Understanding the biology of angiogenesis: review of the most important molecular mechanisms. Blood Cells Mol. Dis. 39, 212–220.

Patel, C.B., Cohen, D.M., Ahobila-Vajjula, P., Sundberg, L.M., Chacko, T., and Narayana, P.A. (2009). Effect of VEGF treatment on the blood-spinal cord barrier permeability in experimental spinal cord injury: Dynamic contrast-enhanced magnetic resonance imaging. J. Neurotrauma 26, 1005–1016.

Peng, X.M., Zhou, Z.G., Glorioso, J.C., Fink, D.J., and Mata, M. (2006). Tumor necrosis factor-alpha contributes to below-level neuropathic pain after spinal cord injury. Ann. Neurol. 59, 843–851.

Profyris, C., Cheema, S.S., Zang, D., Azari, M.F., Boyle, K., and Petratos, S. (2004). Degenerative and regenerative mechanisms governing spinal cord injury. Neurobiol. Dis. 15, 415–436.

Reulen, H.J., Graham, R., Spatz, M., and Klatzo, I. (1977). Role of pressure gradients and bulk flow in dynamics of vasogenic brain edema. J. Neurosurg. 46, 24–35.

Reulen, H.J. (1976). Vasogenic brain oedema. New aspects in its formation, resolution and therapy. Br. J. Anaesth. 48, 741–752.

Rivlin, A.S., and Tator, C.H. (1977). Objective clinical assessment of motor function after experimental spinal cord injury in the rat. J. Neurosurg. 47, 577–581.

Rosenstein, J.M., and Krum, J.M. (2004). New roles for VEGF in nervous tissue—beyond blood vessels. Exp. Neurol. 187, 246–253.

Sharma, H.S. (2005). Pathophysiology of blood-spinal cord barrier in traumatic injury and repair. Curr. Pharm. Des. 11, 1353–1389.

Sondell, M., Lundborg, G., and Kanje, M. (1999). Vascular endothelial growth factor has neurotrophic activity and stimulates axonal outgrowth., enhancing cell survival and Schwann cell proliferation in the peripheral nervous system. J. Neurosci. 19, 5731–5740.

Sondell, M., Sundler, F., and Kanje, M. (2000). Vascular endothelial growth factor is a neurotrophic factor which stimulates axonal outgrowth through the flk-1 receptor. Eur. J. Neurosci. 12, 4243–4254.

Song, S.K., Sun, S.W., Ramsbottom, M.J., Chang, C., Russell, J., and Cross, A.H. (2002). Dysmyelination revealed through MRI as increased radial (but unchanged axial) diffusion of water. Neuroimage 17, 1429–1436.

Song, S.K., Yoshino, J., Le, T.Q., Lin, S.J., Sun, S.W., Cross, A.H., and Armstrong, R.C. (2005). Demyelination increases radial diffusivity in corpus callosum of mouse brain. Neuroimage 26, 132–140.

Storkebaum, E., Lambrechts, D., and Carmeliet, P. (2004). VEGF: Once regarded as a specific angiogenic factor, now implicated in neuroprotection. Bioessays 26, 943–954.

Sundberg, L.M., Herrera, J.J., and Narayana, P.A. (2010). In vivo longitudinal MRI and behavioral studies in experimental spinal cord injury. J. Neurotrauma 27, 1753–1767.

Tammela, T., Enholm, B., Alitalo, K., and Paavonen, K. (2005). The biology of vascular endothelial growth factors. Cardiovasc. Res. 65, 550–563.

Twisk, J., and de Vente, W. (2002). Attrition in longitudinal studies. How to deal with missing data. J. Clin. Epidemiol. 55, 329–337.

van Neerven, S., Joosten, E.A., Brook, G.A., Lambert, C.A., Mey, J., Weiss, J., Marcus, M.A., Steinbusch, H.W., van Kleef, M., Patijn, J., and Deumens, R. (2010). Repetitive intrathecal VEGF165 treatment has limited therapeutic effects after spinal cord injury in the rat. J. Neurotrauma 27, 1781–1791.

Weirich, S.D., Cotler, H.B., Narayana, P.A., Hazle, J.D., Jackson E.F., Coupe, K.J., McDonald, C.L., Langford, L.A., and Harris, J.H., Jr. (1990). Histopathologic correlation of magnetic resonance imaging signal patterns in a spinal cord injury model. Spine 15, 630–638.

Widenfalk, J., Lipson, A., Jubran, M., Hofstetter, C., Ebendal, T., Cao, Y., and Olson, L. (2003). Vascular endothelial growth factor improves functional outcome and decreases secondary degeneration in experimental spinal cord contusion injury. Neuroscience 120, 951–960.

Woods, R.P., Grafton, S.T., Holmes, C.J., Cherry, S.R., and Mazziotta, J.C. (1998). Automated image registration: I. General methods and intrasubject, intramodality validation. J. Comput. Assist. Tomogr. 22, 139–152.

Yashon, D., Bingham, W.G., Jr., Faddoul, E.M., and Hunt, W.E. (1973). Edema of the spinal cord following experimental impact trauma. J. Neurosurg. 38, 693–697.

Ye, F., and Xiang, Q.-S. (2007). Digital tuning to suppress ghost artifacts in EPI by minimization of total variation, in: The International Society for Magnetic Resonance in Medicine. Berlin, Germany, p. 1841.

Zachary, I. (2005). Neuroprotective role of vascular endothelial growth factor: signalling mechanisms, biological function, and therapeutic potential. Neurosignals 14, 207–221.

Zhang, Z.G., Zhang, L., Jiang, Q., Zhang, R., Davies, K., Powers, C., Bruggen, N., and Chopp, M. (2000). VEGF enhances angiogenesis and promotes blood-brain barrier leakage in the ischemic brain. J. Clin. Invest. 106, 829–838.

Address correspondence to:
Ponnada A. Narayana, Ph.D.
Department of Diagnostic and Interventional Imaging
University of Texas Medical School at Houston
6431 Fannin Street
Houston, TX 77030

E-mail: ponnada.a.narayana@uth.tmc.edu